Continuously varying exponents in $A+B\rightarrow 0$ reaction with long-ranged attractive interaction

Sungchul Kwon, S. Y. Yoon, and Yup Kim
Department of Physics and Research Institute of Basic Sciences, Kyung Hee University, Seoul 130-701, Korea
(Received 20 March 2006; published 8 August 2006)

We investigate kinetics of $A+B\rightarrow 0$ reaction with long-range attractive interaction $V(r)\sim -r^{-2\sigma}$ between A and B or with drift velocity $v\sim r^{-\sigma}$ in one dimension, where r is the closest distance between A and B. It is analytically shown that dynamical exponents for density of particles (ρ) and size of domains (ℓ) continuously vary with σ when $\sigma<\sigma_c=1/2$, while that for the distance between adjacent opposite species (ℓ_{AB}) varies when $\sigma<\sigma_c^{AB}=7/6$. For $\sigma>\sigma_c^{AB}$ diffusive motions dominate the kinetics. These anomalous behaviors with the two crossover values of σ are supported by numerical simulations.

DOI: 10.1103/PhysRevE.74.021109 PACS number(s): 64.60.Ht, 05.40.−a, 05.70.Ln

I. INTRODUCTION

The irreversible two-species reaction $A+B\rightarrow 0$ has been intensively and widely investigated as a basic model for various phenomena in physics [1,2], chemistry [3], and biology [4]. When an A and a B particle meet, they instantly and irreversibly combine to form an inert species. Until now the studies for the reaction have been focused on understanding the effect of the fluctuations of the initial particle density or the global bias of particle motions on the kinetics without careful consideration of interaction between A and B even for charged particles [1,5–11]. However, in situations where the kinetics of the reaction is affected by some long-range interaction between A and B such as the Coulomb interaction [12,13], the interaction should be much more important than the simple diffusive motions or global biases to understand the kinetics. Such situations may include matter-antimatter annihilation in the universe, soliton-antisoliton recombination, charge recombination in clouds [14] and electron-hole recombination in irradiated semiconductor structures [9].

It has recently been shown through a simple model that the underlying attractive interaction between opposite species leads to completely different scaling behaviors from those studied so far [12]. In the model, the fluctuation-dominated kinetics leads to the segregation of alternating A-rich and B-rich domains as usual [6]. In addition, domain-boundary particles feel the attractive interaction and are assumed to move to the adjacent opposite species domain with a constant drift velocity. Since the bias is a constant regardless of the distance between A and B, the interaction strength in the model [12] is *infinite*. In contrast the particles inside the domain are screened by the same neighboring particles and the motion of bulk particles is naturally assumed to be isotropic diffusion. As a result, the interaction causes the alternatively changing bias at domain boundaries which is neither the relative nor the uniform bias [6,11] [see Fig. 1(a)].

In noninteracting systems, the density decay has been known to depend on the motion and the mutual statistics of particles. For isotropic diffusions, the particle density $\rho(t)$ scales as $\rho(t)\sim t^{-d/4}$ in d dimensions ($d\leqslant 4$) [5–10]. With the global relative drift, $\rho(t)$ scales as $\rho(t)\sim t^{-(d+1)/4}$ for $d\leqslant 3$ [6]. With the uniform drift of both species, the hard-core (HC) constraint between identical particles leads to the scaling of $\rho(t)\sim t^{-1/3}$ in one dimension [11]. With the infinite interaction, $\rho(t)$ scales as $t^{-d/3}$ regardless of the HC constraint [12]. In one dimension, the uniform bias of HC particles and the infinite interaction lead to the same scaling law for $\rho(t)$, but the scaling behaviors of basic lengths are different. Hence the infinite interaction results in new dynamical scaling behaviors [12].

The constant drift or the infinite attractive interaction is unnatural [12] and cannot explain more general or real situations where the attractive interaction depends on the distance r between A and B. One of the physically realistic attractive interactions is that described by a conserved attractive potential $V(r)\sim -r^{-2\sigma}$. The drift velocity v is then given as $v(r)\sim\sqrt{|V|}\sim r^{-\sigma}$. However in general situations, it is hard to identify the underlying interactions which cause the distant-dependent drift velocity. Hence it is also useful to

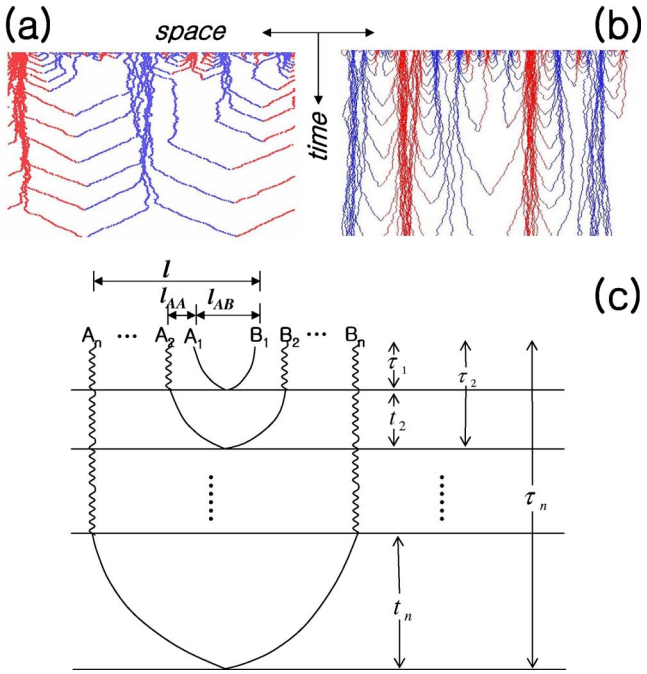

FIG. 1. (Color online) Snapshot of trajectories of $A+B\rightarrow 0$ with the attractive interaction between A and B of (a) $\sigma=0$ and (b) $\sigma=0.3$. (c) The magnified schematic trajectories of adjacent opposite species domains. Subscripts $\{1,2,\ldots,n\}$ indicate the order of the positions of particles from a given domain boundary.

study the kinetics of the reaction with available form of the drift without the informations about the forms of underlying physical interactions.

In this paper, we investigate the kinetics of $A+B\rightarrow 0$ with the drift velocity to opposite species $v(r)\sim r^{-\sigma}$ caused by a certain underlying physical interaction such as $V(r)\sim -r^{-2\sigma}$. In reality the motions of boundary particles cannot be determined only by the interaction, because there should exist various noises, which normally make the background diffusive motions. For this reason, a boundary particle is assumed to stochastically move to its opposite species domain with the rate $p=[1+v(r)]/2$, and to its own domain with $1-p$ during unit time. Hence this model naturally includes the competition between the attractive interaction and the diffusive motion. The drifted motions at boundaries and the competition are expected to lead rich and interesting scaling behavior as σ varies.

Figure 1(b) shows the space-time trajectories for $\sigma=0.3$. Using the trajectories schematically depicted in Fig. 1(c), we analytically derive asymptotic scaling behavior. Intriguingly, we find that all dynamical exponents for various densities and lengths continuously vary when $\sigma<\sigma_c$. Furthermore the scaling behaviors for the present model manifest unique anomalous behaviors, which have not been seen in previous dynamical models with the continuous varying exponents [13,15,16]. The anomalous behavior is that there exist two different crossover values of σ_c. σ_c for the density of particles (ρ) and the size of domains (ℓ) is $\sigma_c=1/2$, while that for the distance between adjacent opposite species (ℓ_{AB}) is $\sigma_c^{AB}=7/6$. Hence the interaction completely changes the scaling behavior of kinetics when $\sigma<\sigma_c^{AB}$. However, when $\sigma\geqslant\sigma_c^{AB}$, the kinetics for diffusive motions is completely recovered [9]. As in the $\sigma=0$ case, the HC constraint is irrelevant due to the isotropic diffusions inside domains. We also numerically confirm our analytical results.

The remainder of this paper is organized as follows. We introduce our model and derive asymptotic scaling behavior of various densities and lengths in Sec. II. We also present Monte Carlo simulation results in Sec. III and finally conclude in Sec. IV.

II. MODEL AND ANALYTICAL APPROACHES

We consider the irreversible reaction $A+B\rightarrow 0$ on one-dimensional lattice with and without hard-core (HC) constraint between identical particles.

With the equal initial density $\rho_A(0)=\rho_B(0)$, particles are randomly distributed on a one-dimensional lattice of size L. When the selected particle has two opposite species neighbors such as $(A\cdots A\cdots B)$, the central particle (A) hops to the opposite species (B) with rate $p=[1+v(r)]/2$ and to the same species (A) with rate $1-p$, where $v(r)=r^{-\sigma}$ and r is the distance between A and B. Otherwise, particles diffuse isotropically. In the region of a length ℓ, the number of A species is initially $N_A=\rho_A(0)\ell\pm\sqrt{\rho_A(0)\ell}$ and the same for N_B. After a time $t\sim\ell^z$, particles travel throughout the whole of the region, and annihilate by pairs. The residual particle number is the number fluctuation in the region, so we have the relation $N_A\sim\sqrt{\ell}$ or $\rho_A\sim 1/\sqrt{\ell}$ for a given length ℓ and the same for N_B and ρ_B [5,6]. As the system evolves, the system becomes a collection of alternating A-rich and B-rich domains. To characterize the structure of segregated domains, we introduce three length scales as in Ref. [9]. The domain length ℓ is defined as the distance between the first particles of adjacent opposite species domains [9]. The length ℓ_{AB} is defined as the distance between two adjacent particles of opposite species, while $\ell_{AA}(\ell_{BB})$ is the distance between adjacent $A(B)$ particles. These lengths scale asymptotically as

$$\ell\sim t^{1/z},\quad \ell_{AA}\sim t^{1/z_{AA}},\quad \ell_{AB}\sim t^{1/z_{AB}}. \tag{1}$$

A bulk particle inside single species domains diffuses isotropically and the mean position of the bulk particle is not substantially changed until it becomes a boundary particle. Once it becomes a boundary particle, it drifts to its neighboring opposite species with velocity $v(r)$ until it annihilates in the midway between two opposite species domains. From this situation in mind we now analytically calculate the scaling behaviors of the kinetics when the drift velocity is $v(r)\sim r^{-\sigma}$. For an AB pair, the time interval for annihilation of the pair is $\tau_{AB}\simeq\ell_{AB}/v(\ell_{AB})\sim\ell_{AB}^{\sigma+1}$. For $\sigma\geqslant 0$, the space-time trajectories of particles are arch-shaped. In the $\sigma=0$ case the trajectories are very close to the pentagon [12]. These arch-shaped trajectories should be self-similar (self-affine) fractal structures, because they should have the scaling symmetry due to the power-law scaling behavior (1). A typical base unit of the self-similar arch-shaped trajectories of adjacent opposite domains are schematically depicted in Fig. 1(c). This base unit allows us to calculate a time τ_ℓ needed to remove the unit of size ℓ surrounded by one scale larger ones. Then the size of the larger unit increases by ℓ during τ_ℓ and we have

$$d\ell/dt\sim\ell/\tau_\ell, \tag{2}$$

which gives the dynamic exponent z. In the following calculations, we consider only the mean positions of bulk particles, and assume $\ell_{AA}(t)$ to be a constant during the annihilation of the base unit. After a smaller unit is completely annihilated, the remainder of the particles redistribute over the larger unit increased by the size of the annihilated unit. Hence we approximate $\ell_{AA}(t)=\cdots=\ell_{AA}(t+\tau_n)=\cdots=\ell_{AA}(t+\tau_\ell)$ during the annihilation of a smaller unit.

As only boundary particles of each domain have two opposite species neighbors, the annihilation of boundary particles comes from the attractive interaction. It takes a time $\tau_1=\ell_{AB}^{\sigma+1}$ for the first boundary pair A_1B_1 in Fig. 1(c), to annihilate. The second pair A_2B_2 isotropically diffuses during time τ_1 until A_1 and B_1 annihilate. After the time τ_1, the second pair becomes a new boundary pair, and the time $t_2\sim(\ell_{AB}+\ell_{AA})^{\sigma+1}$ is needed for the annihilation. So it takes the time $\tau_2\sim\tau_1+t_2$ in total for the second pair to annihilate. Similarly, the nth pair will annihilate after $\tau_n\sim\tau_{n-1}+t_n$, where $t_n=[\ell_{AB}+(n-1)\ell_{AA}]^{\sigma+1}$ for $n\geqslant 2$. From the recurrence relation of τ_n, we find

$$\tau_n \sim \ell_{AB}^{\sigma+1} + \sum_{k=1}^{n-1} (\ell_{AB} + k\ell_{AA})^{\sigma+1}$$
$$\sim \ell_{AB}^{\sigma+1} + [(\ell_{AB} + n\ell_{AA})^{\sigma+2} - \ell_{AB}^{\sigma+2}]/\ell_{AA}. \quad (3)$$

The second line is obtained by integrating out the summation over k. As the number of particles N_ℓ and the length ℓ_{AA} scale as $N_\ell \sim \sqrt{\ell}$ and $\ell_{AA} \sim 1/\rho \sim \sqrt{\ell}$, the time τ_ℓ needed to annihilate the domain of size ℓ in the base unit is given by

$$\tau_\ell \sim \ell_{AB}^{\sigma+1} + [(\ell_{AB} + \ell)^{\sigma+2} - \ell_{AB}^{\sigma+2}]/\sqrt{\ell}. \quad (4)$$

Because of $\ell > \ell_{AB}$ by definition, we finally find the leading scaling of τ_ℓ as

$$\tau_\ell \sim \ell^{\sigma+3/2}, \quad (5)$$

and z is given as $z=\sigma+3/2$ from Eq. (2). Intriguingly, z increases continuously and linearly with σ. However z cannot increase beyond the upper bound $z_c=2$, because domains cannot spread more slowly than those of random diffusion. Hence for $\sigma \geqslant \sigma_c=1/2$, we have $z=2$ regardless of σ. The scaling of ℓ_{AA} is easily obtained from the relation $\ell_{AA} \sim \sqrt{\ell} \sim t^{1/z_{AA}}$. One finds $z_{AA}=2z=2\sigma+3$. Since ℓ_{AA} with the diffusion only scales as $\ell_{AA} \sim t^{1/4}$ [9], the critical value of σ is also $\sigma_c^{AA}=1/2$. For ℓ_{AB}, we consider the change of density during time τ_{AB} [9]. During τ_{AB}, one pair AB annihilates only between boundaries, the change of particle density is given as $d\rho/dt \sim -\rho_{AB}/\tau_{AB}$, where ρ_{AB} is the density of AB pairs. Using relations, $\rho \sim 1/\sqrt{\ell}$, $\rho_{AB}=1/\ell$, and $\tau_{AB} \sim \ell_{AB}^{\sigma+1}$, one finds $\ell_{AB} \sim t^{1/z_{AB}}$ with $z_{AB}=z=\sigma+3/2$. Interestingly, ℓ_{AB} follows the scaling of ℓ. However, ℓ_{AB} with the diffusion only scales as $\ell_{AB} \sim t^{3/8}$ [9] and thus σ_c of ℓ_{AB} is $\sigma_c^{AB}=7/6$. The scaling exponents of three lengths and their critical values of σ, beyond which the diffusive scaling behaviors recover, are summarized as follows:

$$z=\sigma+3/2, \quad z_{AA}=2z, \quad z_{AB}=z,$$
$$\sigma_c=1/2, \quad \sigma_c^{AA}=1/2, \quad \sigma_c^{AB}=7/6. \quad (6)$$

From the scaling of lengths, asymptotic decays of various densities can be extracted. The densities of total particles ($\rho=2\rho_A$), adjacent pairs of same species ($\rho_{AA}=\rho_{BB}$) and adjacent pairs of opposite species (ρ_{AB}) scale as

$$\rho \sim t^{-\alpha}, \quad \rho_{AA} \sim t^{-\alpha_{AA}}, \quad \rho_{AB} \sim t^{-\alpha_{AB}}. \quad (7)$$

As $\rho \sim 1/\sqrt{\ell}$, we have $\rho \sim t^{-1/2z}$ with $\alpha=1/2z=1/(2\sigma+3)$. ρ_{AA} follows the same scaling of ρ due to $\rho_{AA} \sim 1/\ell_{AA} \sim 1/\sqrt{\ell}$ so $\rho_{AA} \sim t^{-\alpha}$ with $\alpha_{AA}=\alpha$. Finally ρ_{AB} scales as $\rho_{AB} \sim 1/\ell$, which leads to $\rho_{AB} \sim t^{-1/z}$ with $\alpha_{AB}=1/z=1/(\sigma+3/2)$. As densities with the diffusion only scale as $\rho \sim \rho_{AA} \sim t^{-1/4}$ and $\rho_{AB} \sim t^{-1/2}$, the upper bound of σ is $\sigma_c=1/2$ for all densities. All decay exponents of various densities are simply given as

$$\alpha=1/2z, \quad \alpha_{AA}=\alpha, \quad \alpha_{AB}=1/z, \quad (8)$$

and σ_c for all densities is $\sigma_c=1/2$. For $\sigma=0$, all the scaling behaviors of the constant drift are fully recovered [12]. As shown in Eqs. (6) and (8), there exist two different crossover values of σ, $\sigma_c(=\sigma_c^{AA})=1/2$ and $\sigma_c^{AB}(=7/6)$, where $\sigma_c < \sigma_c^{AB}$.

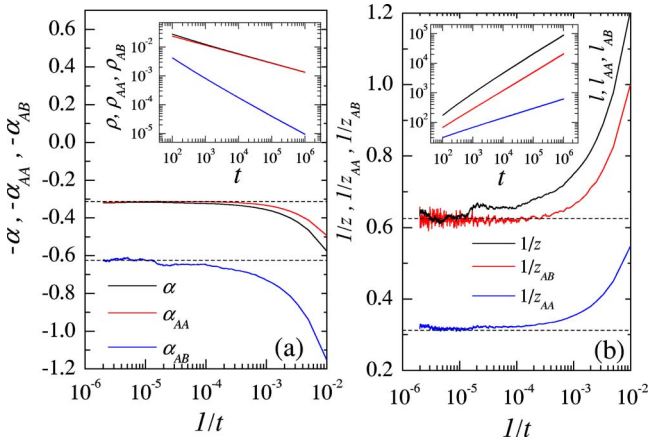

FIG. 2. (Color online) Effective exponents of densities (a) and lengths (b) of the model with HC constraint for $\sigma=0.1$. In each panel, two horizontal lines from top to bottom show the predictions (a) $\alpha=0.313$ and $\alpha_{AB}=0.63$, (b) $1/z=0.625$ and $1/z_{AA}=0.313$.

It is very peculiar that there exist two crossover values. However, the inequality $\sigma_c < \sigma_c^{AB}$ directly comes from the anomalous scaling of ℓ_{AB} only with diffusion. With diffusion only, adjacent opposite domains are effectively repulsive by preferential annihilations of nearby AB pairs. Hence, opposite species pairs are further apart than the typical interparticle distance ℓ_{AA} and, as a result, ℓ_{AB} increases anomalously as $t^{3/8}$ [9]. This anomalous scaling behavior of ℓ_{AB} leads to $\sigma_c < \sigma_c^{AB}$. As the strength of the interaction becomes weak, the effect of the random fluctuation by diffusion becomes strong. The competition between the fluctuation by diffusion and the drift by the interaction leads to the continuously decaying exponents and the critical values of σ above which diffusive motions dominate the kinetics. On the other hand, since the interaction maintains the Galilean invariance of the domain structure, the predictions (6) and (8) are expected to be independent of the HC constraint.

III. MONTE CARLO SIMULATIONS

To confirm our analytic results numerically, we now present the simulation results. With $\rho_A(0)=\rho_B(0)$, A and B particles distribute randomly on a chain of size L. In the simulations we consider both HC particles and the particles without the HC constraint, which we call bosonic particles. In the model with HC particles there can be at most one particle of a given species on a site. In the bosonic model there can be many identical particles on a site. All the simulations are done on the chain of size $L=3\times10^6$ and with $\rho_A(0)=\rho_B(0)=0.1$. We average densities and lengths over 100 independent runs. Figure 2(a) shows densities (inset) and their effective exponents defined as $-\alpha(t)=\ln[\rho(2t)/\rho(t)]/\ln 2$ for $\sigma=0.1$ case of HC particles. We estimate $\alpha=0.317(5)$, $\alpha_{AA}=0.3125(25)$, and $\alpha_{AB}=0.625(25)$, respectively. All results agree well with the prediction (8); $\alpha=\alpha_{AA}=0.3125$ and $\alpha_{AB}=0.625$ for $\sigma=0.1$. Figure 2(b) shows the various lengths and their effective exponents defined as $1/z(t)=\ln[\ell(2t)/\ell(t)]/\ln 2$ for $\sigma=0.1$.

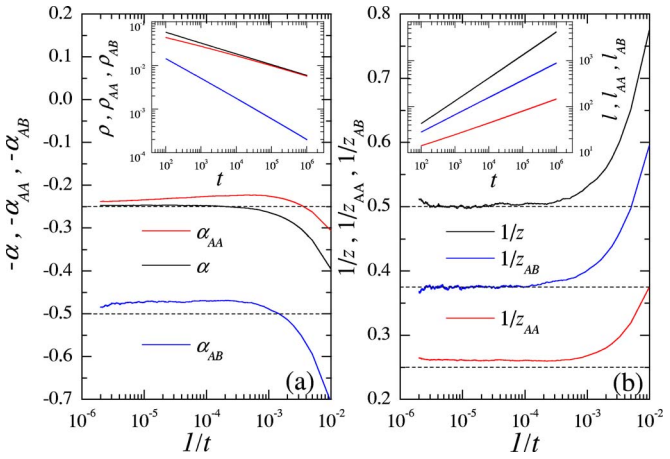

FIG. 3. (Color online) Effective exponents of densities (a) and lengths (b) of the model with HC constraint for $\sigma=1.25$. In each panel, horizontal lines from top to bottom show the prediction (a) $\alpha=\alpha_{AA}=1/4$ and $\alpha_{AB}=1/2$, (b) $1/z=1/2$, $1/z_{AB}=3/8$, and $1/z_{AA}=1/4$.

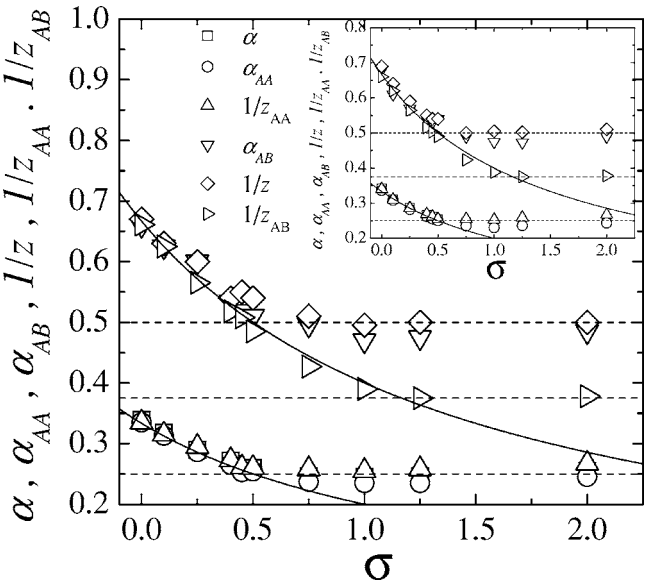

FIG. 4. Plot of dynamical exponents versus σ. Main (inset) plot show the exponents for HC (bosonic) particles. Solid lines in each panel from top to bottom correspond to the predictions; $1/z_{AB}=1/(\sigma+3/2)$ and $1/z_{AA}=1/(2\sigma+3)$. Horizontal dashed lines from top to bottom correspond to $1/z=1/2$, $1/z_{AB}=3/8$, and $1/z_{AA}=1/4$, respectively.

We estimate $z=1.60(5)$, $z_{AA}=3.20(5)$, and $z_{AB}=1.60(5)$ which also agree well with the prediction (6); $z=1.6$, $z_{AA}=3.2$, and $z_{AB}=1.6$ for $\sigma=0.1$. For bosonic particles, we also obtain nearly the same results.

To check the crossover from the continuously varying dynamical scaling to the diffusive one, we now present the numerical results of HC particles for $\sigma=1.25$ $(>\sigma_c^{AB}>\sigma_c)$ in Fig. 3. We estimate $\alpha=0.25(1)$, $\alpha_{AA}=0.24(1)$, and $\alpha_{AB}=0.47(1)$, which agree well with those for the diffusion; $\alpha=\alpha_{AA}=1/4$ and $\alpha_{AB}=1/2$ [9]. For lengths, we estimate $1/z=0.50(5)$, $1/z_{AA}=0.26(1)$, and $1/z_{AB}=0.375(5)$ which also agree well with those for the diffusion, $1/z=1/2$, $1/z_{AA}=1/4$, and $1/z_{AB}=3/8$ [9]. In Figs. 2 and 3, data becomes noisy when the asymptotic scaling regime is reached. The noise can be reduced by averaging more samples. Especially the step of $1/z$ in Fig. 2 just comes from the fluctuation of data so it will disappear for larger samples. The step can be more smooth if we use $m=5$ or 10 instead of $m=2$ in the definition of the effective exponent.

We plot the estimates of all exponents versus σ and the lines for the predictions (6) and (8) both for HC particles and for bosonic particles in Fig. 4. All exponents except $1/z_{AB}$ continuously vary along the predicted lines for $\sigma<\sigma_c=1/2$. In contrast $1/z_{AB}$ varies along the predicted line for $\sigma<\sigma_c^{AB}=7/6$. Beyond σ_c (or σ_c^{AB}), each exponent takes the value of the diffusive system without the interaction regardless of σ. The exponents for HC particles are nearly identical to those for the bosonic particles, and this result comes from the irrelevance of the HC constraint to the kinetics due to the isotropic diffusion inside domains.

IV. SUMMARY AND DISCUSSION

In summary, we investigate the kinetics of irreversible reaction $A+B\to 0$ with the drift velocity $v(r)\sim r^{-\sigma}$ to opposite species at segregated domain boundaries. The drift leads to arch-shaped space-time trajectories of particles from which we analytically derive asymptotic scaling behaviors, and numerically confirm them. Intriguingly, the drift results in continuously varying scaling behavior up to the certain critical values, σ_c (or σ_c^{AB}), above which diffusive motions dominate the kinetics. In our derivations, we only consider the mean positions of particles and neglect the expansion of domains by the random fluctuations during the annihilations of domains. From the irrelevance of HC constraint to the kinetics due to the isotropic diffusion inside domains, the dynamical critical property is independent of HC constraint.

It is worthy to compare the present model with the model of Ref. [13] which considers repulsive force $F\sim r^{-\lambda}$ between the same species as well as the attractive force $F\sim -r^{-\lambda}$ between opposite species. In this model, a particle interacts with all other particles in the system which are HC particles. This model is also shown to have the continuously varying dynamical exponents with λ when $\lambda<2$. Especially, in the range of $\lambda>1$, a boundary particle only interacts with particles in the nearest neighboring domains and the interaction with other particles can be neglected. As the distance between domains (ℓ_{AB}) and the interparticle distance (ℓ_{AA}) are assumed to be the same, the force acting on a boundary particle scales as $F\sim \ell_{AA}\sim\sqrt{\ell}$. As a result, the boundary particles effectively interact with the nearest neighboring particles. Hence, the kinetics for $\lambda>1$ is essentially determined by the motions of particles at domain boundaries as in our model.

For particles undergoing overdamped noiseless motion, this model gives the same exponents for some densities and lengths as those of our models for $\lambda>1$. As λ is given as $\lambda=2\sigma+1$ for the conserved force, the dynamic exponents, $z_{AA}=\lambda+2$ and $z=1+\lambda/2$ of Ref. [13] recover z_{AA} and z of Eq. (6) of our model. Hence the decay exponents of ρ and

ρ_{AA} of both models are also the same. For $\lambda > 2$, the kinetics is also known to be dominated by diffusive motions [13] so the upper bound $\lambda_c = 2$ corresponds to $\sigma_c = 1/2$ of ℓ and ℓ_{AA} in our model.

This model shares some essential features of our model in the range $\lambda > 1$, but it has not considered some features such as two crossover values of λ, the anomalous scaling behavior of ℓ_{AB} and the irrelevance of hard-core constraint. Our model captures the essential features of the oppositely chargedparticle system in which the interaction between opposite charges is weaker than Coulomb interaction in one dimension.

ACKNOWLEDGMENT

This work is supported by Grant No. R01-2004-000-10148-0 from the Basic Research Program of KOSEF.

[1] A. A. Ovchinnikov and Ya. B. Zeldovich, Chem. Phys. **28**, 215 (1978).
[2] P. G. de Gennes, J. Chem. Phys. **76**, 3316 (1982).
[3] N. G. van Kampen, *Stochastic Processes in Physics and Chemistry* (North-Holland, Amsterdam, 1981).
[4] A. M. Turing, Philos. Trans. R. Soc. London, Ser. B **237**, 37 (1952).
[5] D. Toussaint and F. Wilczek, J. Chem. Phys. **78**, 2642 (1983).
[6] K. Kang and S. Redner, Phys. Rev. Lett. **52**, 955 (1984); K. Kang and S. Redner, Phys. Rev. A **32**, 435 (1985).
[7] G. Zumofen, A. Blumen, and J. Klafter, J. Chem. Phys. **82**, 3198 (1985).
[8] S. Cornell, M. Droz, and B. Chopard, Physica A **188**, 322 (1992).
[9] F. Leyvraz and S. Redner, Phys. Rev. A **46**, 3132 (1992).
[10] B. P. Lee and J. Cardy, J. Stat. Phys. **80**, 971 (1995).
[11] S. A. Janowsky, Phys. Rev. E **51**, 1858 (1995); I. Ispolatov, P. L. Krapivsky, and S. Redner, *ibid.* **52**, 2540 (1995).
[12] S. Kwon, S. Y. Yoon, and Y. Kim, Phys. Rev. E **73**, 025102(R) (2006).
[13] I. Ispolatov and P. L. Krapivsky, Phys. Rev. E **53**, 3154 (1996).
[14] K. Lindenberg, B. J. West, and R. Kopelman, Phys. Rev. Lett. **60**, 1777 (1988).
[15] B. P. Lee and J. L. Cardy, Phys. Rev. E **48**, 2452 (1993); A. D. Rutenberg and A. J. Bray, *ibid.* **50**, 1900 (1994); T. Ohta and H. Hayakawa, Physica A **204**, 482 (1994).
[16] H. Hinrichsen, Adv. Phys. **49**, 815 (2000); D. ben-Abrahan, V. Privman, and D. Zhong, Phys. Rev. E **52**, 6889 (1995).